

A Mathematical Treatment of the Effect of Particle Size Distribution on Mass Transfer in Dispersions

BENJAMIN GAL-OR and H. E. HOELSCHER

Johns Hopkins University, Baltimore, Maryland

A mathematical model is proposed that takes into account interaction between drops or bubbles in a swarm as well as the effect of particle size distribution. The model is used to solve the equations for unsteady state mass transfer with and without chemical reaction when the drops or bubbles are suspended in a nonextraordinarily purified agitated fluid. Steady state diffusion to a family of moving drops with clean interface and without interaction and chemical reaction has been also analyzed. The model demonstrates the sort of error that may arise when one applies uniform drop size assumptions to drop populations. It is shown quantitatively that this error is usually small when one replaces the variable particle size by the mean. By using variables that can be determined and predicted, the equations presented permit the estimation of diffusion rate per unit area of interface, as well as the average concentration and the total average rate of mass transfer in the disperser under pseudo steady state conditions.

Recent studies on heat and mass transfer to and from drops or bubbles in continuous media have primarily been limited to studies of the transfer mechanism for single moving drops or bubbles. Transfer to or from swarms of drops or bubbles moving in an arbitrary fluid field is very complex and has been analyzed theoretically only in certain simple cases. To achieve a useful analysis the assumption is commonly made that the drops or bubbles are of uniform size. This permits calculation of the total interfacial area of the dispersion, the contact time of the particle, and the transfer coefficient based on the average size. However, it is well known that the particle size distribution is not uniform and the assumption of uniformity may lead to error. Of particular importance is the effect of coalescence and breakup of drops or bubbles and its effect on the particle size distribution. Thus a theoretical expression for the effect of particle size distribution would be of assistance in the interpretation of mass transfer data and the prediction of equipment performance. A particle size distribution function recently proposed by Bayens (12) has proved useful for many liquid-liquid and gas-liquid systems and for hydrosols coagulating in Brownian motion. This function will be used in the following evaluation of the total mass transfer rate in the vessel. Prior to this, we shall first examine the transfer rate per unit area at the particle surface as a function of the particle size as predicted by two models proposed for single as well as for swarms of drops or bubbles.

DIFFUSIONAL FLUX AS A FUNCTION OF PARTICLE SIZE (DIFFUSION TO A SINGLE MOVING DROP WITH A CLEAN INTERFACE UNDER STEADY STATE CONDITION WITHOUT CHEMICAL REACTION)

Let us first consider the diffusional flux to a clean surface of a small single drop falling in a liquid medium. Let the drop under consideration be falling under the influence of gravity in a system of immiscible liquids that have different densities.

Levich (23) has analyzed this problem by solving the equation for convective diffusion in spherical coordinates for that component which dissolves in the continuous phase when the average value of the thickness of the diffusion boundary layer is much smaller than the drop diameter. Levich considered only diffusion to a drop of sufficiently small dimensions, so that Reynolds number is substantially less than unity. Nevertheless, the Peclet number may be sufficiently large so that a diffusion boundary layer is formed near the surface of the drop. Using the stream function Levich has demonstrated that the diffusional flux to the surface of the drop is given by

$$N_A^* = \left[\frac{D \mu_c U}{2a(\mu_c + \mu_d)} \right]^{1/2} \sqrt{\frac{3}{\pi}} \sqrt{\frac{(1 + \cos \theta)^2}{2 + \cos \theta}} (c_o - c_i) \quad (1)$$

This flux is proportional to the square root of the drop velocity and inversely proportional to the square root of the drop radius. However, U is also a function of the radius of the drop. To evaluate the average diffusional flux as a function of drop size, the total mass transfer rate from the entire surface of the drop will be divided by the entire surface of the drop

$$\bar{N}_A = \frac{\int_0^{2\pi} \int_0^\pi N_A^* a^2 \sin \theta d\phi d\theta}{4\pi a^2} = \frac{2}{\sqrt{6}\pi} \left[\frac{D \mu_c U}{a(\mu_c + \mu_d)} \right]^{1/2} (c_o - c_i) \quad (2)$$

To evaluate \bar{N}_A as a function of a alone the Rybczynski-Hadamard formula (16, 17)

$$U = \frac{2|\rho_d - \rho_c|g a^2}{3\mu_c} \cdot \frac{\mu_c + \mu_d}{2\mu_c + 3\mu_d} \quad (3)$$

(derived from the Navier-Stokes equation) will be used for this case.

H. E. Hoelscher is with the University of Pittsburgh, Pittsburgh, Pennsylvania.

It is clear that the Rybczynski-Hadamard equation becomes the Stokes equation

$$U = \frac{2}{g} \cdot \frac{|\rho_d - \rho_c| g a^2}{\mu_c} \quad (4)$$

when $\mu_d \gg \mu_c$

By substituting Equation (3) into Equation (2) we obtain

$$\bar{N}_A = \frac{2}{3\sqrt{\pi}} \left[\frac{D|\rho_d - \rho_c|g}{2\mu_c + 3\mu_d} \right]^{1/2} (c_o - c_i) \sqrt{a} \quad (5)$$

Equation (5) shows the influence of densities and viscosities of both phases on the average mass transfer rate per unit area. In addition, this equation predicts that the average diffusional flux is proportional to the square root of the radius of the drop. Thus a smaller drop which is moving slower has a smaller flux than the bigger drop that moves faster.

For the calculation of the total average rate of transfer from a population of drops having a distribution of sizes, the integration over the entire surface of the drop family should be evaluated. This will be done later. Note, however, that there is ample evidence for the presence of minute amounts of surface active impurities in all but the most extraordinarily purified systems and these can have a profound effect (decrease) on drop velocity and on the rate of transfer from the interface. Thus the above equations serve only for the extreme case of a steady flow around a single small drop moving in extraordinarily purified systems. It does not provide for any interaction between drops in a swarm.

UNSTEADY STATE MASS TRANSFER WITH AND WITHOUT CHEMICAL REACTION (TRANSFER FROM A SWARM OF BUBBLES OR DROPS MOVING IN AGITATED FLUID WITH INTERACTION IN THE PRESENCE OF SURFACTANTS)

Proposed Model

Certain hydrodynamical problems, as well as mass transfer problems in the presence of surface active agents, have been investigated theoretically under steady state conditions (1 to 3). However, if we take into account the fact that in this case the nonstationary term must appear in the equation of mass transfer, it becomes apparent that an exact analysis is possible if a mixing-contacting mechanism is adopted instead of a theoretical stream line flow around a single drop or bubble sphere.

The surfactants that are present in practical systems tend to form some kind of skin around the bubble or drop which effectively retards the movement of the surface elements of the continuous phase adjacent to the interface. Talc particles sprinkled on the surface become virtually immobile if the surface is even slightly contaminated, indicating that the surface elements are stagnant and are setting up a considerable resistance to the clearing of the surface by eddies of liquid approaching obliquely (7). This may be the reason why mass and heat transfer coefficients are *unaffected* by the amount of mechanical power dissipated in mixing of the dispersion (4). According to Garner et al. (5, 6) and Davies and Mayer (11), the control of mass transfer changes from surface renewal to diffusion through a stagnant film in the presence of surfactants. Consequently, the actual mechanism under these conditions may be in some agreement with the behavior of the surface elements that were proposed by Toor and Marchello in their film-penetration model (24). The contact time of these surface elements may be as long as the residence time of the drop or bubble in the dispersion or, in other words, from the moment of drop or bubble formation until it bursts on the free surface of the dispersion. When the bubble or drop bursts on the free

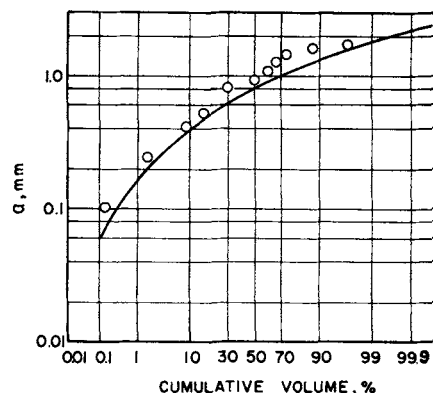


Fig. 1. Comparison of accumulative distribution of Equation (6) with typical data of drop size distribution in liquid-liquid dispersion produced in a rotating disk contactor (15). Dispersed phase: white oil; continuous phase: water; $\alpha = 2.13 \text{ mm.}^{-2}$ (for $a_{32} \cong a_v$).

surface of the dispersion, the surface elements remain and are mixed with the continuous phase. These assumptions, coupled with interaction effects between adjacent particles in a swarm, may give a better approximation to the actual mechanism in practical systems (especially for moderate or high dispersed phase holdups) than the assumptions of a steady theoretical stream line flow around a single sphere. Thus, for the purpose of this analysis, a type of a film-penetration, mixing-contacting mechanism will be considered coupled with the effects of particle size distribution and dispersed phase holdup.

A simplified theoretical model that takes into account the interaction between bubbles (or drops) as a function of dispersed phase holdup and under pseudo steady state mass transfer with and without simultaneous chemical reaction was recently proposed by Gal-Or and Resnick (13, 14, 23) and a modification of its principles and mathematical equations will be used here for studying the effect of particle size on the diffusional flux.

The system now to be considered is a semibatch system in which the dispersed phase is continuously fed into a batch of continuous phase under constant operating conditions. Under these pseudo steady state conditions, the bubble or drop average residence time in the continuous phase is $\bar{\theta}$ and their size distribution is independent of time. We assume the particle size distribution function $f(a, \alpha)$ to be that proposed by Bayens (12):

$$f(a, \alpha) = 4 \left(\frac{\alpha^3}{\pi} \right)^{1/2} a^2 \exp(-\alpha a^2) \quad (6)$$

in which

$$\alpha = \left(\frac{16\sqrt{\pi} N_v}{3\Phi} \right)^{2/3} > 0 \quad (7)$$

This equation has been checked in a batch system in which α changes with time because the coagulation rate changes the ratio of N_v/Φ in time. The agreement of this equation with experimental data of Swift and Friedlander (19) is excellent. For semibatch and continuous systems under constant operating conditions the rate of agitation, coalescence, and breakup of drops or bubbles is constant and consequently $f(a, \alpha)$ is not a function of time. The ratio N_v/Φ is constant (but different) for each operating condition. Consequently Equations (6) and (7) were checked against the experimental data of Olney (15) for several liquid-liquid dispersions (Figure 1) and with a gas-liquid dispersion produced in this laboratory in a new type of gas-liquid contactor (Figure 2) (25). The agreement in both cases is good. The deviations observed

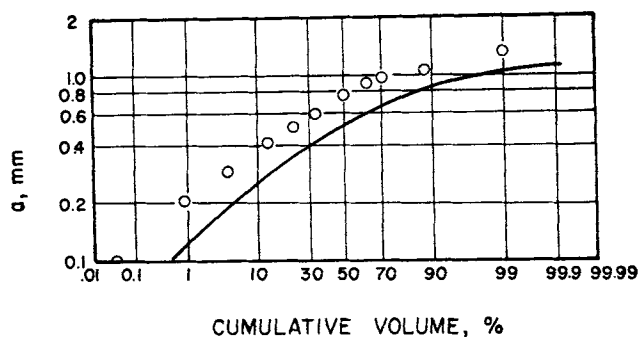


Fig. 2. Comparison of accumulative distribution of Equation (6) with typical data of bubble size distribution in gas-liquid dispersion produced in a new kind of contactor without pressure drop per stage (25). Dispersed phase: air; continuous phase: water; $\alpha = 4.62 \text{ mm.}^{-2}$.

result probably from distortion of the bubbles and drops from spherical shape and a departure from random collisions, coalescence, and breakup. Equation (6) is a type of normalized gamma distribution function, that is

$$\int_0^{\infty} f(a, \alpha) da = 1 \quad (8)$$

and is of the same type as the Maxwell-Boltzman speed distribution of gaseous atoms.

The concentration of particles in the dispersion will be evaluated for our purpose in terms of the average particle size in the system; thus

$$N_v = \frac{\Phi}{4/3 \pi \bar{a}_v^3} \quad (9)$$

in which \bar{a}_v is the mean volume radius defined by (see Appendix)

$$\bar{a}_v = \sqrt[3]{\frac{\sum n_i a_i^3}{\sum n_i}} \quad (10)$$

With the use of Equation (9), Equation (7) gives

$$\alpha = \left(\frac{4}{\sqrt{\pi} \bar{a}_v^3} \right)^{2/3} \quad (11)$$

or

$$f(a, \alpha) = f^*(a, \bar{a}_v) = \frac{16}{\pi \bar{a}_v^3} a^2 \exp \left[- \left(\frac{4}{\sqrt{\pi} \bar{a}_v^3} \right)^{2/3} a^2 \right] \quad (12)$$

Equation (12) indicates that the entire distribution may be determined if one parameter \bar{a}_v is known as a function of the physical properties of the system and the operating variables. It is constant for a particular system under constant operating conditions. For a batch system, \bar{a}_v changes with time of contact due to coalescence, etc.

The total volume of the dispersion (or of the reactor) will be subdivided into many subvessels (or subreactors). In each, a fraction of the total number of particles having a radius between a and $a + da$ will be considered. The distribution of particles in the subreactors will be given by $f^*(a, \bar{a}_v)$, as described qualitatively in Figure 3. For simplicity we take all particles in any subreactor to have average radius a , that is, $[a + (a + da)]/2 \rightarrow a$. The dispersed phase volume in any subreactor is thus given by

$$V_v d\Phi = \frac{4}{3} \pi a^3 N_v V_v f^*(a, \bar{a}_v) da \quad (13)$$

because

$$\Phi = \frac{4}{3} \pi N_v \int_0^{\infty} a^3 f^*(a, \bar{a}_v) da \quad (14)$$

In each subreactor the volume of the continuous phase V_j is subdivided again into a number of equal-volume elements u_L equivalent to the number of drops or bubbles in the subreactor. Each drop or bubble is then considered to be enveloped by a spherical shell of volume u_L . Thus

$$u_L = \frac{4 V_j \pi a^3}{3 Q_j \bar{\theta}_j} = \frac{4}{3} \pi (b_j^3 - a^3) \quad (15)$$

where b_j is equal to the outer radius of the shell. From Equation (15) b_j is expressed as

$$b_j = a \left(1 + \frac{V_j}{Q_j \bar{\theta}_j} \right)^{1/3} \quad (16)$$

in which $\bar{\theta}_j$ is a function of operating and system variables. In each subreactor the dispersed phase holdup fraction should be the same as the overall fraction Φ ; thus[†]

$$b_j = a \Phi^{-1/3} \quad (17)$$

Consequently, for the same fractional holdup there are more particles per unit volume as the particle size decreases, causing b_j (which is a yardstick for the distance between the particles) to decrease, resulting in more and more interaction between adjacent particles. This is one type of interaction that is taken into account in this model.

Each drop or bubble in each subreactor is now assumed to be introduced into each element for a retention time equal to the average residence time of the drops or bubbles in the continuous phase. At $t = \bar{\theta}$ the particle is removed and the continuous phase in the shell is completely mixed and another particle is introduced. Thus, the total number of operating models is equal to the total number of drops or bubbles in the disperser. This is similar to the model proposed by Gal-Or and Resnick (13, 14). Changing agitation intensity, for example, will change Φ , $\bar{\theta}$, and \bar{a}_v and consequently the b_j distribution, mass fluxes, and the total interfacial area are changed. Thus, the effects of operating and system variables are indirectly interacting in this semidynamic model.

The equation for unsteady state chemical reaction and diffusion through the stagnant elements of this semidynamic model is

$$D \nabla^2 c = kc + \frac{\partial c}{\partial t} \quad (18)$$

Equation (18) in spherical coordinates becomes

$$D \left[\frac{1}{r^2} \frac{\partial}{\partial r} \left(r^2 \frac{\partial c}{\partial r} \right) \right] = kc + \frac{\partial c}{\partial t} \quad (19)$$

since by symmetry

$$\frac{\partial c}{\partial \theta} = \frac{\partial c}{\partial \phi} = 0 \quad (20)$$

[†] That means also that b_j distribution is about of the same type as $f^*(a, \bar{a}_v)$ distribution.

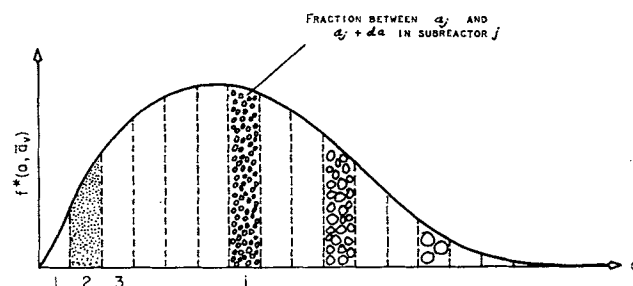


Fig. 3. Distribution of particles in the model of subreactors as a function of $f^*(a, \bar{a}_v)$.

The initial condition should take into account the effect of mixing under these pseudo steady state conditions; thus

$$\text{at } t = 0, c = c_o \text{ for } a < r \leq b_j \quad (21)$$

The boundary conditions are

$$\text{at } r = a, c = c_i \text{ for } t \geq 0 \quad (22)$$

For the boundary condition at b_j , we shall use the fact that, no matter can diffuse through the outer boundary in the model, thus

$$\text{at } r = b_j, \frac{\partial c}{\partial r} = 0 \text{ for } t \geq 0 \quad (23)$$

These boundary conditions are more accurate for very small values of a than the boundary conditions used in a previous model (13, 14). Note, however, that the second boundary condition does not imply that the profiles of concentrations are unaffected by the distance between adjacent particles as expressed in Equation (17). The solution of Equation (19) with Equations (21) to (23) is (23)

$$c = \frac{c_i a}{r} \cdot \frac{\cosh \left[(b_j - r) \sqrt{\frac{k}{D}} \right] - \frac{1}{b_j} \sqrt{\frac{D}{k}} \sinh \left[(b_j - r) \sqrt{\frac{k}{D}} \right]}{\cosh \left[(b_j - a) \sqrt{\frac{k}{D}} \right] - \frac{1}{b_j} \sqrt{\frac{D}{k}} \sinh \left[(b_j - a) \sqrt{\frac{k}{D}} \right]} +$$

$$+ \frac{1}{r} \sum_{n=1}^{\infty} \left(c_o - \frac{c_i \lambda_n^2}{\lambda_n^2 + k/D} \right) \frac{2a \sin [\lambda_n (r - a)] \exp [-(\lambda_n^2 D + k) t]}{\lambda_n \{ b_j \sin^2 [\lambda_n (b_j - a)] - a \}} \quad (24)$$

in which λ_n are the positive roots of

$$\lambda_n b_j = \tan [\lambda_n (b_j - a)] \quad (25)$$

According to the mechanisms of the model the following mass balance is made at $t = \bar{\theta}$ before and after the complete mixing of the model to evaluate c_o :

$$\int_{\bar{a}_v}^{\bar{b}} 4 \pi r^2 c(r, \bar{\theta}) dr = \int_{\bar{a}_v}^{\bar{b}} 4 \pi r^2 c_o dr \quad (26)$$

in which

$$\bar{b} = \bar{a}_v \Phi^{-1/3} \quad (26A)$$

By integrating and rearranging, one obtains the final result

criteria $\bar{\theta}$, \bar{a}_v , and Φ that can be considered as indirect interaction parameters between drops or bubbles in swarm. However, $\bar{\theta}$, for example, can include effects other than interaction such as mixing. Actually, for a given system, these parameters are a function of the operating variables. Practically, Equation (27) can be used for an estimation of the average concentration of the dissolved component in a semibatch disperser.

The instantaneous rate of diffusing matter per unit surface area of particle having radius a will be thus given by

$$N_{Aj} = -D \left(\frac{\partial c}{\partial r} \right)_{r=a} = \frac{D}{a} \left[\frac{c_i}{\Omega} \left\{ (1 - \Phi^{1/3}) \cosh \xi + \left(\sqrt{\frac{k}{D}} a - \frac{\Phi^{1/3}}{a} \sqrt{\frac{D}{k}} \right) \sinh \xi \right\} \right. \\ \left. - 2 \sum_{n=1}^{\infty} \left(c_o - \frac{c_i \lambda_n^2}{\lambda_n^2 + k/D} \right) \frac{\exp [-(\lambda_n^2 D + k) t]}{\Phi^{-1/3} \cdot \sin^2 [\lambda_n a (\Phi^{-1/3} - 1)] - 1} \right] \quad (29)$$

in which

$$\xi = a (\Phi^{-1/3} - 1) \sqrt{\frac{k}{D}} \quad (29A)$$

$$\Omega = \cosh \xi - \frac{\Phi^{1/3}}{a} \sqrt{\frac{D}{k}} \sinh \xi \quad (29B)$$

The dependence of the instantaneous diffusional flux on the particle size for various chemical reaction rates and for $t = 0.001, 0.01$ and $t = \bar{\theta} = 2.85$ sec. was calculated with the IBM 7094 computer. The result is shown in Figure 4. For a fast chemical reaction ($k = 10^4$ sec.⁻¹), N_{Aj} is not a function of time because the gradient is very steep and is formed almost instantaneously. As the chemical reaction rate decreases, N_{Aj} decreases too. However, for smaller chemical reaction rates there is an observed influence of time. As t increases N_{Aj} decreases. For most of the practical region of particle sizes, N_{Aj} does not change as a changes. However, for very small a values, N_{Aj} tends to increase slightly and then reaches a maximum and decreases. This phenomenon may be explained in terms of

$$\left(\sqrt{\frac{k}{D}} \bar{a}_v - \frac{\Phi^{1/3}}{\bar{a}_v} \sqrt{\frac{D}{k}} \right) \tanh \bar{\xi} + 1 - \Phi^{1/3} \left[1 - \frac{\Phi^{1/3}}{\bar{a}_v} \sqrt{\frac{D}{k}} \tanh \bar{\xi} \right] - 2 \sum_{n=1}^{\infty} \frac{\exp [-(\lambda_n^2 D + k) \bar{\theta}] \left[1 - \Phi^{-1/3} \cos \bar{\eta} \right]}{(\lambda_n^2 + k/D) (\Phi^{-1/3} \sin^2 \bar{\eta} - 1)}$$

$$\frac{\bar{a}_v^2}{3} \left(\frac{1}{\Phi} - 1 \right) - 2 \sum_{n=1}^{\infty} \frac{\exp [-(\lambda_n^2 D + k) \bar{\theta}] \left[1 - \Phi^{-1/3} \cos \bar{\eta} + \frac{\sin \bar{\eta}}{\lambda_n \bar{a}_v} \right]}{(\lambda_n^2 + k/D) (\Phi^{-1/3} \sin \bar{\eta} - 1)}$$

in which

$$\bar{\xi} = (\bar{b} - \bar{a}_v) \sqrt{\frac{k}{D}} = \bar{a}_v (\Phi^{-1/3} - 1) \sqrt{\frac{k}{D}}, \\ \bar{\eta} = \lambda_n \bar{a}_v (\Phi^{-1/3} - 1) \quad (28)$$

The whole continuous phase is mixed so c_o is equal in all subreactors and is thus expressed in terms of the overall

two opposing effects. The first is the curvature effect that increases the diffusional flux as a decreases. The second effect is the interaction between adjacent particles. For a given contact time and holdup b_j (which is a yardstick for the distance between adjacent particles) decreases as a decreases, causing the diffusional flux to decrease with decreasing a . The last process begins to control the rate at sufficiently small values of a . As the chemical reaction

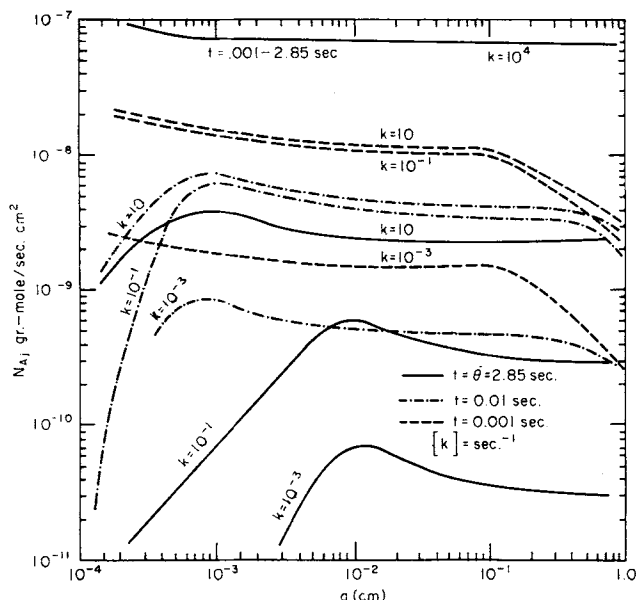


Fig. 4. Influence of particle size on instantaneous mass transfer rates per unit surface area as affected by interaction between particles (as function of a in subreactors and for constant dispersed phase holdup), chemical reaction rates, and contact times. c_o was calculated from Equation (27) and N_{Aj} from Equation (29). $c_i = 1.46 \times 10^{-7}$ g.-mole/sec., $D = 2.3 \times 10^{-5}$ sq. cm./sec., $\Phi = 0.064$, $\bar{a}_v = 0.1$ cm., $\bar{\theta} = 2.85$ sec.

rate decreases, this maximum in N_{Aj} moves to higher values of a as a result of a deeper penetration of diffused matter as k decreases. In other words, for smaller chemical reaction rates the interaction between adjacent particles will start to control at higher particle sizes than for high chemical rates.

EFFECT OF PARTICLE SIZE DISTRIBUTION ON TOTAL DIFFUSION RATE

Moving Drops with Clean Interface under Steady State Without Interaction

To evaluate the total rate of mass transfer in the whole vessel \bar{N}_T , an integration over the entire surface of the swarm of drops with size distribution $f^*(a, \bar{a}_v)$ must be done. Thus

$$\bar{N}_T = \int_0^A \bar{N}_A dA \quad (30)$$

From Equation (5) we have

$$\bar{N}_A \propto a^{1/2}$$

In addition, dA should be expressed as a function of the particle size distribution.

With the subreactors model discussed in the previous section we have

$$dA = \frac{4\pi a^2 V_v}{4/3\pi a^3} d\Phi = \frac{3V_v}{a} d\Phi \quad (31)$$

The use of Equations (9) and (13), Equation (31) gives

$$dA = \frac{3\Phi V_v}{\bar{a}_v^3} a^2 f^*(a, \bar{a}_v) da \quad (32)$$

or

$$\bar{N}_T = \frac{2}{3\sqrt{\pi}} \left[\frac{D|\rho_d - \rho_c|g}{2\mu_c + 3\mu_d} \right]^{1/2} (c_o - c_i) \frac{3\Phi V_v}{\bar{a}_v^3} \cdot 4 \left(\frac{\alpha^3}{\pi} \right)^{1/2} \int_0^\infty a^{4.5} e^{-\alpha a^2} da \quad (33)$$

There is a maximum and minimum particle size in any particle distribution and the limits on the integration would preferably be these limits. However, in examining the accumulative density of particles via the distribution function, we obtain

Accumulative density, % =

$$100 \left\{ 1 - 4 \left(\frac{\alpha^3}{\pi} \right)^{1/2} \int_a^\infty a^2 e^{-\alpha a^2} da \right\} = 100 \left\{ \text{erf} [\sqrt{\alpha} a] - 2 \left(\frac{\alpha}{\pi} \right)^{1/2} a e^{-\alpha a^2} \right\} \quad (34)$$

For $\bar{a}_v = 0.12$ cm., for example, the cumulative vol. % of particles with $0.02 \leq a \leq 0.2$ cm. covers 0.6% to 95.4% and for particles with $0.01 \leq a \leq 0.3$ cm. between 0.06% to 99.956%. Thus evaluation of the integral in Equation (33) gives

$$\bar{N}_T = \frac{4}{\pi} \left[\frac{D|\rho_d - \rho_c|g}{2\mu_c + 3\mu_d} \right]^{1/2} \cdot \frac{\Phi V_v}{\bar{a}_v^3} \cdot \frac{\Gamma(2.75)}{\alpha^{5/4}} (c_o - c_i) \quad (35)$$

or

$$k_L a^* = \frac{4}{\pi} \left[\frac{D|\rho_d - \rho_c|g}{2\mu_c + 3\mu_d} \right]^{1/2} \cdot \frac{\Phi}{\bar{a}_v^3} \cdot \frac{\Gamma(2.75)}{\alpha^{5/4}} \quad (36)$$

By substituting Equation (11) in Equation (36) we finally obtain

$$k_L a^* = 1.04 \frac{\Phi}{\sqrt{\bar{a}_v}} \left[\frac{D|\rho_d - \rho_c|g}{2\mu_c + 3\mu_d} \right]^{1/2} \quad (37)$$

It is sometimes more convenient to express Equation (37) by using a_{32} instead of \bar{a}_v . For this case (see Appendix)

$$\bar{a}_v = \frac{1}{1.148} a_{32} = 0.872 \frac{\sum n_i a_i^3}{\sum n_i a_i^2} \quad (38)$$

The interfacial area per unit volume is

$$a^* = \frac{\int_0^A dA}{V_v} = \frac{3\Phi}{\bar{a}_v^3} \int_0^\infty a^2 \frac{16}{\pi \bar{a}_v^3} a^2 \exp \left[- \left(\frac{4}{\sqrt{\pi} \bar{a}_v^3} \right)^{2/3} a^2 \right] da \quad (39)$$

$$\therefore a^* = 0.872 \frac{3\Phi}{\bar{a}_v} = \frac{3\Phi}{a_{32}} \quad (40)$$

Consequently

$$k_L = 0.371 \left[\frac{D|\rho_d - \rho_c|g}{2\mu_c + 3\mu_d} \right]^{1/2} \sqrt{a_{32}} \quad (41)$$

It is of interest to compare Equation (41) with the general experimental correlations proposed by Calderbank and Moo-Young (4) for heat and mass transfer in gas-liquid, liquid-liquid, and solid-gas dispersions, in which the dispersed phases are "free to move under the influence of gravity" (4) and also with data on transfer by free convection from spheres. For average bubble diameters less than about 0.25 cm. they report

$$k_L = 0.31 \left[\frac{|\rho_c - \rho_d| \mu_c g}{\rho_c^2} \right]^{1/3} \left[\frac{D \rho_c}{\mu_c} \right]^{2/3} \quad (42)$$

and for bubble swarms of average bubble diameter greater than about 0.25 cm. they correlated the data as

$$k_L = 0.42 \left[\frac{|\rho_c - \rho_d| \mu_c g}{\rho_c^2} \right]^{1/3} \left[\frac{D \rho_c}{\mu_c} \right]^{1/2} \quad (43)$$

Calderbank and Moo-Young (4) have also reported some typical data for transition from large bubble mass transfer coefficients to small bubble values (see Figure 5). As stated above, they give two different correlations for small and large diameters; however the data show that

$$k_L \propto (a)^{1/2}$$

as predicted by Equation (41). By applying Equation (41) for Calderbank's system and by using his data for D , ρ , μ , and bubble diameter (22, 4), the comparison is shown in Figure 5, indicating that the large and small bubbles, including the transition region, are generally predicted by Equation (41). This result does give higher values, in particular for the water-glycerol system containing lower concentration of glycerol.

It should be mentioned, however, that in making this experimental comparison we have assumed that the suspended particles entrained by turbulent eddies and which thus describe complicated trajectories in the fluid are moving relative to the fluid at a slip velocity U given by Equation (3). This is only an approximation. However, to be more accurate we must consider real systems in which the relative velocity of the particles relative to the fluid is strongly influenced by small traces of surface-active agents that are present in all but the most extraordinarily purified systems. Under these conditions, as stated above, the surface-active agents form some kind of skin around the bubble or drop that effectively retards internal circulation and may reduce U to the Stokes' range for solid particles, thus causing k_L to decrease, respectively (5 to 11). In a recent experimental study (18) the average relative velocities of air bubbles to water-glycerol solutions in a mechanically agitated vessel were found to be in the range of Stokes' law. By using these data it is found that $Re < 1$ only for the experimental results of very small bubbles and high concentration of glycerol (see Figure 5). This result may explain part of the increased disagreement between Equation (41) (which requires that Reynolds number be small) and the experimental results for larger bubbles and lower concentrations of glycerol. Unsteady state effects are also a possible source of complicating factors. Another effect that

contributes to the increased agreement for high viscosity is the theoretical conclusion of Levich (3) that adventitious surfactant impurities will not influence transfer when the viscosity is high. Calderbank and Moo-Young's work was probably influenced by very small traces of surfactant impurities that are present, as stated above, in all but the most extraordinarily purified systems.

This case can also be approached with Kolmogorev's theory of local isotropic turbulence to predict the velocity of suspended particles relative to a homogeneous and isotropic turbulent flow. By examination of this situation for spherical particles moving with a constant relative velocity, U varying randomly in direction, Levich (3) has demonstrated that

$$U = \frac{2}{3\sqrt{3}} \cdot \frac{|\rho_d - \rho_c|}{\rho_c} \cdot \frac{\epsilon_o^{3/4}}{\nu^{5/4}} a^2 \quad (44)$$

This is valid for a particle whose size is substantially less than the scale of an inner turbulent zone λ_o and whose relative velocity is smaller than the velocity V_λ of turbulent eddies of scale λ . Therefore, the Reynolds number $\frac{Ua}{\nu} < \frac{V_{\lambda o} \lambda_o}{\nu} \sim 1$. Equation (44) means that the particle

motion is quasi steady as if it were moving in some other steady acceleration field, for example, in a gravitational field. Substitution of Equation (44) into Equation (2) and integration as in Equation (33) will give the same dependency on a as in Equations (35) to (41). The final result is

$$k_L = 0.287 \left[\frac{D|\rho_d - \rho_c|}{(\mu_d + \mu_c)\nu_c^{1/4}} \right]^{1/2} \epsilon_o^{3/8} \sqrt{a} \quad (45)$$

For this case, however, k_L is expressed in terms of ϵ_o , the intensity of turbulence or power per unit mass which is proportional to $N^3 D_i^2$ for mechanically agitated vessels. Calderbank and Moo-Young (4), however, found that mass and heat transfer coefficients are unaffected by the mechanical power dissipated in the system. According to Equation (45) this may be the case when the product $\epsilon_o^{3/8} \sqrt{a}$ remains constant.

Considering the effect of particle size distribution on the mass transfer coefficient, Equation (5) should be compared with Equation (41). By evaluating k_L from Equation (5) the result is

$$k_L = 0.379 \left[\frac{D|\rho_d - \rho_c|g}{2\mu_c + 3\mu_d} \right]^{1/2} \sqrt{a} \quad (46)$$

This result indicates that if the varying particle size a is replaced by the mean a_{32} , the result would not be much different from that derived by using the particle size distribution. It is of interest to compare this result to the work of Hanratty (20), who showed that if other distribution functions are employed instead of an average contact time it is usually found that the results are not markedly affected by the form of distribution function used.

The reason for the small effect in our case is due to the small difference between the 4.5 exponent in the integral of Equation (33) and the 4.0 exponent in the integral of Equation (39).

Swarms of Bubbles or Drops with Interaction Between Them under Pseudo Steady State Conditions (Mass Transfer and Chemical Reaction)

By noting that c_o is a function of \bar{a}_v and not of a , the total rate of mass transfer in the vessel is obtained from Equations (29), (30), (32) and (12):

$$N_T = \frac{48 \Phi V_v D}{\pi \bar{a}_v^6} \int_0^\infty a^3 \cdot \exp[-\alpha a^2]$$

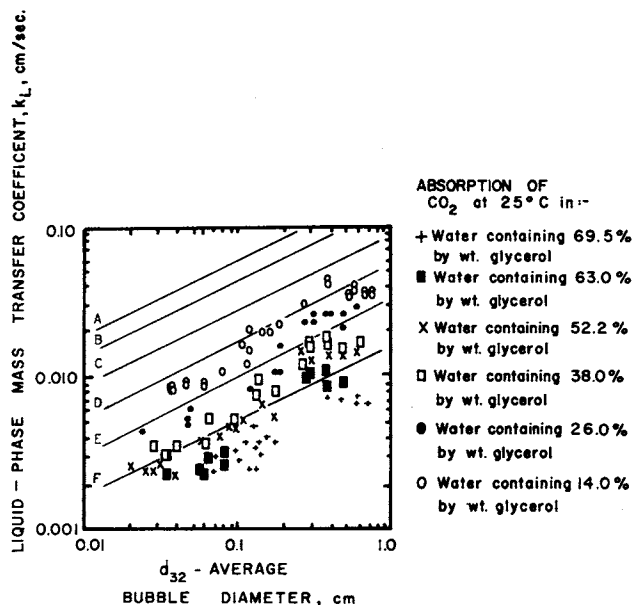


Fig. 5. Typical data of Calderbank and Moo-Young (4) for mass transfer coefficients as a function of bubble surface mean diameter. The lines represent Equation (41) for the following concentrations of glycerol: A-14.0%, B-26.0%, C-38.0%, D-52.2%, E-63.0%, F-69.5%.

$$\left\{ \frac{\frac{\omega-1}{\omega} \cosh \left[a(\omega-1) \sqrt{\frac{k}{D}} \right] \cdot c_i}{\cosh \left[a(\omega-1) \sqrt{\frac{k}{D}} \right] - \frac{1}{a\omega} \sqrt{\frac{D}{k}} \sinh \left[a(\omega-1) \sqrt{\frac{k}{D}} \right]} + \frac{c_i \left(\sqrt{\frac{k}{D}} a - \frac{1}{a\omega} \sqrt{\frac{D}{k}} \right) \sinh \left[a(\omega-1) \sqrt{\frac{k}{D}} \right]}{\cosh \left[a(\omega-1) \sqrt{\frac{k}{D}} \right] - \frac{1}{a\omega} \sqrt{\frac{D}{k}} \sinh \left[a(\omega-1) \sqrt{\frac{k}{D}} \right]} - 2 \sum_{n=1}^{\infty} \left(c_o - \frac{c_i \lambda_n^2}{\lambda_n^2 + k/D} \right) \cdot \frac{\exp [-(\lambda_n^2 D + k) t]}{\omega \cdot \sin^2 [\lambda_n a(\omega-1)] - 1} \right\} da \quad (47)$$

in which

$$\omega = \Phi^{-1/3} \quad \omega > 1 \quad (47A)$$

CASE 1

Fast Chemical Reaction

For this case $k \gg 1$

$$\cosh \left[a(\omega-1) \sqrt{\frac{k}{D}} \right] \rightarrow \sinh \left[a(\omega-1) \sqrt{\frac{k}{D}} \right]$$

(Note: $\cosh x \rightarrow \sinh x$ when $x > 3$). $c_o \rightarrow 0$ and Equation (47) gives

$$N_T = \frac{48 \Phi V_v D}{\pi \bar{a}_v^6} c_i \left[\frac{\omega-1}{\omega} \cdot \frac{1}{2\alpha^2} + \sqrt{\frac{k}{D}} \cdot \frac{\Gamma(2\frac{1}{2})}{2\alpha^{2\frac{1}{2}}} \right] \quad (48)$$

Consequently, for fast chemical reaction rates N_T is not a function of the contact time and $N_T = \bar{N}_T$.

Note: As noted previously in this work the limits of the integral should be from a_{\min} to a_{\max} . However, for simplicity and as an approximation it is evaluated as shown in spite of the fact that a is never zero. This does not seriously affect the numerical result. Substituting Equation (11) into Equation (48) we finally obtain

$$k_L a^* = 2.59 \frac{\Phi D}{\bar{a}_v^2} \left[1 - \Phi^{1/3} + 1.014 \bar{a}_v \sqrt{\frac{k}{D}} \right] \quad (49)$$

or by using Equation (38)

$$k_L a^* = 3.41 \frac{\Phi D}{a_{32}^2} \left[1 - \Phi^{1/3} + 0.885 a_{32} \sqrt{\frac{k}{D}} \right] \quad (49A)$$

By substituting Equation (40), Equation (49A) gives

$$k_L = 1.135 \frac{D}{a_{32}} \left[1 - \Phi^{1/3} + 0.885 a_{32} \sqrt{\frac{k}{D}} \right] \quad (50)$$

The effect of particle size distribution on the mass transfer coefficient will be obtained for this case by using Equation (29) with Equation (17). The result is

$$N_{A_i} = \frac{D c_i}{a} \left[1 - \Phi^{1/3} + a \sqrt{\frac{k}{D}} \right] \quad (51)$$

or

$$k_L = \frac{D}{a_{32}} \left[1 - \Phi^{1/3} + a_{32} \sqrt{\frac{k}{D}} \right] \quad (52)$$

when replacing the variable particle size a with the mean a_{32} . Comparison of Equation (52) with Equation (50)

demonstrates the effect of particle size distribution for this case, that is, interaction between particles as a function of Φ , fast chemical reaction with simultaneous diffusion. This serves to emphasize the error that may arise when one applies uniform drop size assumptions to drop populations. Quantitatively, the error is small because $1 - \Phi^{1/3}$ is small by comparison to the second term in the brackets ($\cdot \cdot k_L \cong \sqrt{k/D}$) and consequently Equation (50) and Equation (52) will give about the same result.

CASE 2

$k = 0$, No Chemical Reaction

In order to maintain c_o constant for this case, a continuous system should be considered (for semibatch systems

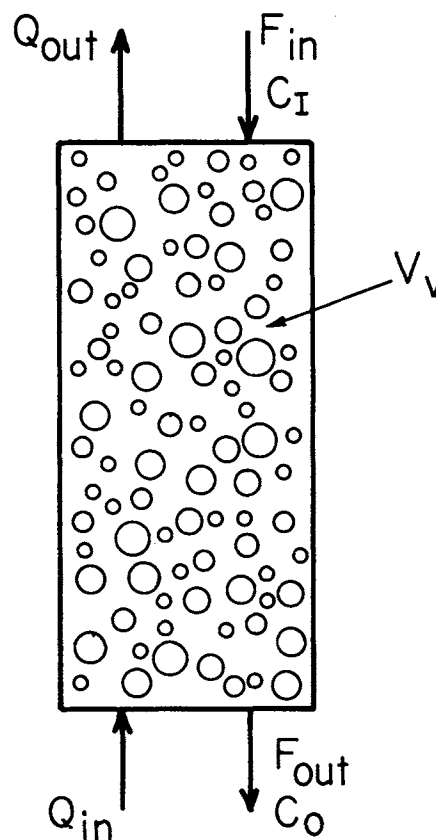


Fig. 6. A stage in a continuous flow system for contacting of two phases (small mass transfer rates, $F_{in} \cong F_{out}$, $Q_{in} \cong Q_{out}$). The dispersion is stirred either artificially or by the particles themselves as they pass through the fluid.

without chemical reaction, the average concentration in the liquid will increase with time until it reaches c_i . For $k = 0$ Equation (24) yields

$$c = c_i + \frac{1}{r} \sum_{n=1}^{\infty} (c_o - c_i) \frac{2a \cdot \sin [\lambda_n (r - a)] \exp [-\lambda_n^2 D t]}{\lambda_n \{b_j \cdot \sin^2 [\lambda_n (b_j - a)] - a\}} \quad (53)$$

To evaluate c_o , a continuous system will be considered as described in Figure 6. c_o is the average overall concentration of the outgoing stream F and should be the same for each of the subreactors because the continuous phase is mixed. The model is described in Figure 7. Thus, the mass balance may be evaluated in terms of \bar{a}_v and $\bar{\theta}$. (c_o should not be a function of a , that is, c_o is the same for any subreactor and consequently may be evaluated in terms of the average overall quantities \bar{a}_v , Φ , and $\bar{\theta}$). Thus

$$\int_{\bar{a}_v}^{\bar{b}} 4\pi c_{(r,\bar{\theta})} r^2 dr = \int_{\bar{a}_v}^{\bar{b}} 4\pi c_o r^2 dr + \frac{F\bar{\theta}}{N} (c_o - c_i) \quad (54)$$

in which

$$\bar{b} = \bar{a}_v \Phi^{-1/3} = \bar{a}_v \omega$$

By integrating and rearranging, the final result is

$$c_o = \frac{\frac{c_i}{3} (\omega^3 - 1) - 2c_i \sum_{n=1}^{\infty} \left[\frac{1 - \omega \cdot \cos \{\lambda_n \bar{a}_v (\omega - 1)\} + \frac{\sin \{\lambda_n \bar{a}_v (\omega - 1)\}}{\bar{a}_v \lambda_n}}{\{\omega \cdot \sin^2 [\lambda_n \bar{a}_v (\omega - 1)] - 1\}} \right] e^{-\lambda_n^2 D \bar{\theta}} + \frac{F c_i}{3Q}}{\frac{\omega^3 - 1}{3} + \frac{F}{3Q} - 2 \sum_{n=1}^{\infty} \frac{[1 - \omega \cdot \cos \{\lambda_n \bar{a}_v (\omega - 1)\} + \sin \{\lambda_n \bar{a}_v (\omega - 1)\} / \bar{a}_v \lambda_n] e^{-\lambda_n^2 D \bar{\theta}}}{\{\omega \cdot \sin^2 [\lambda_n \bar{a}_v (\omega - 1)] - 1\}}} \quad (55)$$

Equation (55) is useful for an estimation of the average concentration in the case of mass transfer without chemical reaction in a continuous flow system.

From Equation (53) we obtain

$$N_{Aj} = -D \left(\frac{\partial c}{\partial r} \right)_{r=a} = \frac{D}{a} (c_i - c_o) \sum_{n=1}^{\infty} \frac{2 \exp [-\lambda_n^2 D t]}{\omega \cdot \sin^2 [\lambda_n a (\omega - 1)] - 1} \quad (56)$$

and

$$N_T = 30.56 \frac{\Phi V_v D}{\bar{a}_v^6 \omega} (c_i - c_o) \cdot \sum_{n=1}^{\infty} \exp [-\lambda_n^2 D t] \int_0^{\infty} \frac{a^3 \exp [-\alpha a^2]}{\sin^2 [\lambda_n a (\omega - 1)] - 1/\omega} da \quad (57)$$

Equation (57) must be solved with a computer and for this reason the limits 0 and ∞ may be replaced by a_{\min} and a_{\max} . The average mass transfer rate at the pseudo steady state conditions is

$$\bar{N}_T = \frac{\int_0^{\bar{\theta}} N_T dt}{\int_0^{\bar{\theta}} dt} \quad (58)$$

Equation (58) is based on the assumption that all particles are in contact for an equal period $\bar{\theta}$, whereas in the

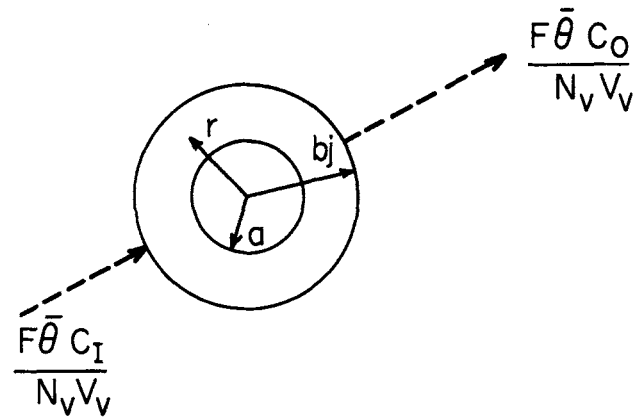


Fig. 7. Spherical two-phase model for subreactor (for the evaluation of c_o ; $a = \bar{a}_v$, $b_j = \bar{b}$).

real system there is a distribution of residence times of which $\bar{\theta}$ is the average. However, experimental results indicate (21) that the instantaneous mass transfer coefficient decreases to an asymptotic value as particle contact time increases and that after 6 sec. the coefficient is practically constant. Thus, most of the mass is transferred during a short initial contact period and particles with a long residence time do not contribute particularly to the total mass transfer. Thus, the error introduced by using

an average residence time is minimal. If other distribution functions are employed it is usually found that the results are not markedly affected by the distribution functions used (20).

By evaluating the integral (58) we obtain

$$\bar{N}_T = 30.56 \frac{\Phi^{4/3} V_v D}{\bar{a}_v^6 \bar{\theta}} (c_i - c_o) \cdot \sum_{n=1}^{\infty} \frac{1}{\lambda_n^2 D} \left(1 - \exp [-\lambda_n^2 D \bar{\theta}] \right) \cdot \int_{a_{\min}}^{a_{\max}} \frac{a^2 \exp [-\alpha a^2]}{\sin^2 [\lambda_n a (\Phi^{-1/3} - 1)] - \Phi^{1/3}} da \cdot \bar{N}_T = \psi'(\Phi, D, a_{32}, \bar{\theta}, V_v, c_i, c_o)$$

in which

$$c_o = \psi''(c_i, F, c_i, Q, D, \Phi, a_{32}, \bar{\theta})$$

Consequently

$$\bar{N}_T = \psi'(V_v, c_i, F, c_i, Q, D, \Phi, a_{32}, \bar{\theta})$$

This case has not been solved numerically because of the excessive number of calculations involved.

CONCLUSIONS

The mathematical model which has been presented accounts for interaction between the drops or bubbles in a

swarm as well as the effect of particle size distribution. The equations were solved for unsteady state mass transfer with and without chemical reaction when the drops or bubbles are suspended in a nonextraordinarily purified agitated fluid. The diffusion to a family of moving drops with clean interface and without interaction and chemical reaction has been also analyzed under steady state conditions.

For semibatch and continuous systems under constant operating conditions and pseudo steady state, the rates of agitation, coalescence, and breakup of drops or bubbles are constant; consequently the particle size distribution is not a function of time and may be estimated by the use of one parameter \bar{a}_v . The change of agitation intensity, for example, changes Φ , $\bar{\theta}$, and \bar{a}_v and accordingly this model predicts the changes in diffusional fluxes. It thus predicts the variations in particle size distribution function, interfacial area, interaction between particles, average concentration, and the total average mass transfer rate in the vessel. The interaction between adjacent particles in the dispersion increases as the dispersed phase holdup fraction increases, causing the distance between adjacent particles to decrease, and resulting in a change of mass transfer rate in the disperser.

The model demonstrates the sort of error that may arise when one applies uniform size assumption to drop populations. It was shown that this error is usually small when the variable particle size is replaced by the mean. By using variables that can be determined and predicted the equations presented permit the estimation of diffusion rate per unit area of interface as well as the average concentration and the total average rate of mass transfer in the dispersion under pseudo steady state conditions. The model proposed here can be adopted for the analogous case of heat transfer in an agitated dispersion.

ACKNOWLEDGMENT

The authors acknowledge their indebtedness to the Allied Chemical Foundation and the National Science Foundation, Division of Engineering, for financial support which made this work possible. Discussions with Charles A. Bayens were helpful, and for his interest the authors are also grateful.

NOTATION

| | |
|---------------------|---|
| a | = radius of drop or bubble |
| a_{32} | = surface mean radius [Equation (A2)] |
| a_j | = radius of particles in subreactors |
| \bar{a}_v | = mean volume radius [Equation (10)] |
| a^* | = specific area of dispersion [Equation (39)] |
| A | = total interfacial area between the dispersed and the continuous phase in a disperser |
| \bar{b} | = average outer radius of model [Equation (26A)] |
| b_j | = outer radius of the model for subreactor j [Equation (17)] |
| c | = concentration of dissolved component |
| c_i | = concentration of dissolved component at the interface |
| c_I | = concentration of dissolved component in the continuous phase entering a continuous flow system |
| c_o | = average concentration of dissolved component in the continuous phase at $t = 0$ after the model is mixed [Equations (27) or (55)]. Concentration at $t \rightarrow \infty$ in Equations (1), (2), (5), (33), and (35) |
| D | = diffusion coefficient |
| D_i | = diameter of mechanical agitator |
| $f(a, \alpha)$ | = particle size distribution function [Equation (6)] |
| $f^*(a, \bar{a}_v)$ | = particle size distribution function [Equation (12)] |

| | |
|-------------|--|
| F | = volumetric flow rate of the continuous phase into a continuous flow system |
| g | = local acceleration |
| k | = first-order reaction rate constant |
| k_L | = average mass transfer coefficient for the continuous phase |
| N | = rotational speed of impeller. Total number of particles in the system |
| N_{Aj} | = instantaneous rate of mass transfer per unit drop or bubble surface area in subreactor j |
| N_A^* | = local rate of mass transfer per unit drop or bubble surface area |
| \bar{N}_A | = average rate of mass transfer per unit drop or bubble surface area |
| N_j | = number of particles in subreactor j |
| N_T | = instantaneous total rate of mass transfer |
| \bar{N}_T | = total average rate of mass transfer in the vessel |
| N_v | = number of drops or bubbles per unit volume of dispersion |
| Q | = volumetric flow rate of dispersed phase |
| r | = radius in spherical coordinates, measured from the center of particle |
| t | = time |
| U | = magnitude of relative velocity of the particle with respect to the continuous phase |
| u_L | = volume of the continuous phase in the model [Equation (15)] |
| V_j | = volume of continuous phase in subreactor j |
| V_r | = radial component of velocity in the continuous phase |
| V_θ | = tangential component of velocity in the continuous phase |
| V_v | = total volume of dispersion or volume of empty vessel of a continuous flow system |

Greek Letters

| | |
|----------------|--|
| α | = variable defined in Equations (7) and (11) |
| λ_n | = roots of Equation (25) |
| Γ | = gamma function |
| ϵ_o | = intensity of turbulence as power per unit mass |
| η | = variable defined in Equation (28) |
| μ | = viscosity |
| ν | = kinematic viscosity |
| ρ | = density |
| ξ | = dimensionless variable [Equation (29A)] |
| $\bar{\xi}$ | = dimensionless variable [Equation (28)] |
| θ | = cone angle between the vector radius and the vertical directed in the sense of the drop motion |
| $\bar{\theta}$ | = average residence time of the bubbles or drops in the continuous phase |
| ϕ | = polar angle in spherical coordinates |
| Φ | = dispersed phase holdup fraction |
| ω | = dimensionless variable = $\Phi^{-1/3}$ |
| Ω | = dimensionless variable [Equation (29B)] |

Subscripts

| | |
|-----|---|
| j | = subreactor |
| c | = continuous phase |
| d | = dispersed phase |
| n | = summation sign of all positive roots of Equation (25) |

LITERATURE CITED

1. Ruckenstein, E., *Chem. Eng. Sci.*, **19**, 131 (1964).
2. Levich, V. G., *Intern. Chem. Eng.*, **2**, 78 (1962).
3. ———, "Physicochemical Hydrodynamics," Prentice Hall, Englewood Cliffs, N. J. (1962).
4. Calderbank, P. H., and M. B. Moo-Young, *Chem. Eng. Sci.*, **16**, 39 (1961).

5. Garner, F. H., and A. B. Hale, *ibid.*, **2**, 157 (1953).
6. Garner, F. H., and T. T. Lane, *Trans. Inst. Chem. Eng. (London)*, **37**, 162 (1959).
7. Davies, J. T., "Advances in Chemical Engineering," pp. 1-50, Academic Press, New York (1963).
8. Savic, P., *Natl. Res. Lab. Rept. (Canada) MT-22* (1953).
9. Kinter, R. C., "Advances in Chemical Engineering," pp. 52-92, Academic Press, New York (1963).
10. Davies, J. T., A. A. Kilmer, and G. A. Ratcliff, *Chem. Eng. Sci.*, **19**, 483 (1964).
11. Davies, J. T., and G. R. A. Mayers, *ibid.*, **16**, 55 (1961).
12. Bayens, C., unpublished paper, Chem. Eng. Dept., Johns Hopkins Univ.
13. Gal-Or, Benjamin, D.Sc. thesis, Technion, Israel Inst. Technol. (in Hebrew) (1964).
14. ———, and William Resnick, *Chem. Eng. Sci.*, **19**, 653 (1964).
15. Olney, R. B., *A.I.Ch.E. J.*, **10**, 827 (1964).
16. Hadamard, J., *Compt. Rend. Acad. Sci. Paris*, **152**, 1735 (1911).
17. Rybczynski, W., *Bull. Intern. Acad. Sci. Cracovie (A)*, **40** (1911).
18. Gal-Or, Benjamin, and William Resnick, *A.I.Ch.E. J.*, **11**, 740 (1965).
19. Swift, I. L., and S. K. Friedlander, *J. Colloid Sci.*, **19**, 621 (1964).
20. Hanratty, T. J., *A.I.Ch.E. J.*, **2**, 359 (1956).
21. Deindoerfer, F. H., and A. Humphrey, *Ind. Eng. Chem.*, **53**, 755 (1961).
22. Calderbank, P. H., *Trans. Inst. Chem. Engrs.*, **37**, 173 (1959).
23. Gal-Or, Benjamin, and William Resnick, *Ind. Eng. Chem. Process Design Development*, **5**, 15 (1966); *ibid.*, to be published.
24. Toor, H. L., and T. M. Marchello, *A.I.Ch.E. J.*, **4**, 97 (1958).
25. Gal-Or, Benjamin, *A.I.Ch.E. J.*, **12**, No. 3 (1966).

APPENDIX

Mean volume radius is defined as

$$a_v = \sqrt[3]{\frac{\sum_{i=1}^{N_v} n_i a_i^3}{\sum_{i=1}^{N_v} n_i}} \quad (A1)$$

However, in many cases the average particle radius is evaluated experimentally by measuring of dispersed phase holdup and total area of dispersed particles A and by expressing the results as

$$a_{32} = \frac{3[\text{Holdup vol.}]}{A} \quad (A2)$$

It should be noted that Equation (A2) gives the surface mean radius which is defined as

$$a_{32} = \frac{\sum_{i=1}^{N_v} n_i a_i^3}{\sum_{i=1}^{N_v} n_i a_i^2} = \frac{3\Phi}{A/V_v} = \frac{3[\text{Holdup vol.}]}{A} \quad (A3)$$

By the use of Equation (14) and (32), Equation (A3) gives

$$a_{32} = \frac{\int_0^\infty a^3 f^\circ(a, \bar{a}_v) da}{\int_0^\infty a^2 f^\circ(a, \bar{a}_v) da} = \frac{\Gamma(3.0)}{\Gamma(2\frac{1}{2})\alpha^{1/2}} = 1.148\bar{a}_v \quad (A4)$$

Manuscript received April 30, 1965; revision received October 4, 1965; paper accepted December 3, 1965. Paper presented at A.I.Ch.E. Philadelphia meeting.

Longitudinal Dispersion in Rotating Impeller Types of Contactors

TERUKATSU MIYAUCHI, HIROMI MITSUTAKE, and ICHIRO HARASE

University of Tokyo, Tokyo, Japan

On the basis of a back-flow model, the rates of interstage mixing of continuous phase for RDC and Mixco columns are measured experimentally under flow and nonflow conditions. These rates are correlated into dimensionless formulas for wide combinations of operational condition, column geometry, and dimensions, and are put into a single formula by introducing the power number as an additional parameter. The final correlation covers the impeller Reynolds number from 3.5×10^3 to 1.0×10^6 and the diameter of columns from 4.1 to 218 cm.

Longitudinal dispersion coefficients for continuous phase in the rotating shaft types of columns have been investigated here experimentally to interpret the extrac-

tion behavior of the contactors along the concept presented for two-phase counterflow operations with longitudinal dispersion (1, 5, 7, 8, 16, 19, 20, 23, 28). Two types of contactors are investigated: the rotating disk contactor (RDC) introduced by Raman and Olney (14), and the Mixco column of Oldshue and Rushton (13).

Hiromi Mitsutake, and Ichiro Harase are with Chiyoda Chemical Engineering and Construction Co., Ltd., Tokyo, Japan.